atmosphere

MDPI

Article

Enhanced Transcriptomic Resilience following Increased Alternative Splicing and Differential Isoform Production between Air Pollution Conurbations

Shenkai Pan [1,†] Xiaokai Feng [2,†] Daniel Pass [3], Rachel Adams [4], Yusong Wang [1], Xuemin Dong [1], Zhenzhen Lin [1], Chunguo Jiang [2], Tim Jones [5], Kelly BéruBé [3,*] and Xiangjiang Zhan [1,*]

[1] Institute Zoology, Chinese Academy of Sciences, 1 Beichen West Road, Chaoyang District, Beijing 100101, China
[2] Department of Respiratory and Critical Care Medicine, Beijing Institute of Respiratory Medicine, Beijing Chao yang Hospital, Capital Medical University, Beijing, 100020, China.
[3] School of Biosciences, Cardiff University, Museum Avenue, PO Box 911, Cardiff CF10 3US, UK
[4] Cardiff School of Health Sciences, Cardiff Metropolitan University, Western Avenue, Cardiff CF5 2YB, UK
[5] School of Earth and Environmental Sciences, Cardiff University, Park Place, Cardiff, CF10 3YE, UK
* Correspondence: berube@cardiff.ac.uk, zhanxj@ioz.ac.cn
† Contributed equally to the manuscript.

Abstract: Adverse health outcomes caused by ambient particulate matter (PM) pollution occur in a progressive process, with neutrophils eliciting inflammation or pathogenesis. We investigated the toxico-transcriptomic mechanisms of PM in real-life settings by comparing healthy residents living in Beijing and Chengde, the opposing ends of a well-recognised air pollution (AP) corridor in China. Beijing recruits (BRs) uniquely expressed ~12,000 alternative splicing (AS)-derived transcripts, largely elevating the proportion of transcripts significantly correlated with PM concentration. BRs expressed PM-associated isoforms (PMAIs) of *PFKFB3* and *LDHA*, encoding enzymes responsible for stimulating and maintaining glycolysis. PMAIs of *PFKFB3* featured different COOH-terminals, targeting PFKFB3 to different sub-cellular functional compartments and stimulating glycolysis. PMAIs of *LDHA* have longer 3'UTRs relative to those expressed in Chengde recruits (CRs), allowing glycolysis maintenance by enhancing *LDHA* mRNA stability and translational efficiency. PMAIs were directly regulated by different *HIF-1A* and *HIF-1B* isoforms. BRs expressed more non-functional *Fas* isoforms and a resultant reduction of intact *Fas* proportion is expected to inhibit the transmission of apoptotic signals and prolong neutrophil lifespan. BRs expressed both membrane-bound and soluble *IL-6R* isoforms instead of only one in CRs. The presence of both *IL-6R* isoforms suggested a higher migration capacity of neutrophils in BRs. PMAIs of *HIF-1A* and *PFKFB3* were down-regulated in Chronic Obstructive Pulmonary Disease patients compared with BRs, implying HIF-1 mediated defective glycolysis may mediate neutrophil dysfunction. PMAIs could explain large variances of different phenotypes, highlighting their potential application as biomarkers and therapeutic targets in PM-induced diseases, which remain poorly elucidated.

Keywords: air pollution; alternate splicing; biomarker; neutrophils; resilience; transcriptome

Citation: Pan, S.; Feng, X.; Pass, D.; Adams, R.; Wang, Y.; Dong, X.; Lin, Z.; Jiang, C.; Jones, T.; BéruBé, K.; et al. Enhanced Transcriptomic Resilience following Increased Alternative Splicing and Differential Isoform Production between Air Pollution Conurbations. *Atmosphere* **2021**, *12*, x. https://doi.org/10.3390/xxxxx

Received: date
Accepted: date
Published: date

1. Introduction

Ambient airborne particulate matter (PM) pollution (i.e. particles with a 50% cut-off aerodynamic diameter of 10 microns; PM10) refers to the miasma of detritus from anthropogenic (e.g. diesel exhaust [DE], coal fly ash (FA) and carbon black (CB) particulates) and natural (e.g. volcanic ash, pollen grains and mineral dusts) sources, and is now considered to be the largest environmental risk factor to human health in the 21st century [1]. It is causally linked by epidemiology to cardio-pulmonary morbidity and mortality [2] and

increases risks for multiple chronic diseases (e.g. chronic obstructive pulmonary disease [3]; COPD), cancer [4] and diabetic syndromes [5]) leading to 7 million [6] (i.e. ~4 million deaths attributed to ambient and ~3 million with household air pollution (AP) recorded deaths annually). Notably, these adverse health effects are reached in a progressive (i.e. chronic) exposure process, rather than intermittent toxic challenges. Inhaled PM can deposit in the alveoli of the lungs and trigger local inflammation, which in turn can lead to systemic inflammation [7]. Inhalation exposure to ambient PM emissions derived from anthropogenic [8-11], biogenic [12], geogenic [13-15] and technogenic [16, 17] sources have been shown to elicit systemic inflammatory responses that establish a primary line of defense against inhaled exogenous environmental particulates. However, long-term exposure may impair this defense line, thus promoting the progression of pathogenesis [18]. As a result, we need to understand how the immune system properly reacts to PM and how this reaction shifts to deleterious responses that comprise the mechanisms underlying how PM puts human health at risk.

Neutrophils account for ~40-60% of the white blood cell (WBC) population, representing the body's primary line of defense when exposed to PM [19]. Recently, it has been recognized that neutrophils play the role of a double-edged sword. When appropriately activated, neutrophils secrete multiple pro-inflammatory cytokines to activate other lymphocytes (e.g. T-cells), along with expressing MHC Class II molecules to present antigen to T-cells [20] and regulate other cell types (e.g. red blood cells; RBC) [21, 22]. Otherwise, they would release large numbers of tissue-damaging molecules, causing inflammation and consequent pathogenesis progression [20]. In this respect, neutrophils serve as a critical checkpoint in responding to PM. There have been human studies of global changes in gene expression using RNA-seq following controlled exposures or using *in* vivo [23] and *in vitro* models [24-26] that have provided some insights. Yet there is a paucity of rigorously assessed investigations regarding the impact of PM on gene expression of neutrophils in 'real-life' settings. Therefore, there is still no concrete biological plausibility to explain the mechanisms underlying how neutrophils protect against PM and/or promote pathogenesis.

In our pilot study, based on a hierarchical design of comparative toxico-transcriptomes and physiological responses, we first characterized the neutrophil gene expression responses produced by alternate splicing (AS) in two groups of healthy city dwellers living at the opposing ends of a well-recognized AP corridor beginning in Beijing (source) and ending in Chengde (sink) [27]. We integrated these data with micro-environmental measures of occupational exposure to three pollutants: (1) Chinese Air Quality Index [AQI]; (2) PM2.5 (particular matter with diameter ≤ 2.5 μm) and; (3) PM10. Moreover, we measured specific soluble inflammatory mediators using enzyme-linked immunosorbent assay (ELISA) to help identify the genes and gene networks differentially activated in response to these exposures. In addition, we investigated the associations between AS-derived isoforms of interest and physiological responses. We believe that AS provides a means of regulating environmental fitness to impart 'resilience' in the face of continuous inhalation exposure challenges to poor air quality. We further compared the AS-derived transcripts between healthy recruits and COPD patients collected in Beijing, providing insight into mechanisms underlying how neutrophil immune function becomes impaired and promotes pathogenesis.

2. Materials and Methods

2.1 Study design

All protocols were ethically approved by the Institute of Zoology Research Ethics Committee (REC), Chinese Academy of Sciences (Beijing) and all methods were performed in accordance with the relevant guidelines and regulations. In order to reduce confounding factors, healthy (i.e. non-smokers with no pre-existing cardiopulmonary disease) recruits were selected, ranging from ages 23 to 39.

Beijing was chosen as the primary, highly polluted urban location since it is one of the most intensely researched cities in the World. Chengde was selected as a comparison site because it is at the end of a recognised geographical AP transportation route, and as such, their PM compositions would be similar. Therefore, we characterized and compared the air quality between the two cities, along with the transcriptomic responses among Beijing recruits (BRs), Chengde recruits (CRs) and COPD patients from Beijing, aiming to determine how transcriptome responds to the air pollution.

2.2. PM Monitoring and Characterization

The daily air quality data of Beijing and Chengde was derived from the Chinese Government AQI website (https://www.aqistudy.cn/). Our previous research [28-35] on the physiochemical characteristics of Beijing AP along with other sources of current literature were utilized for PM characterisation.

2.3. AP Transportation Time Assessment

An indication of the AP transport time can be derived, using the data available from Beijing airports (https://www.aqistudy.cn/), which shows that wind speeds are usually in the range of 6-8 mph, therefore the 110 miles transport to Chengde will take less than one day. The conclusion that Chengde AP has a one-day lag-time from Beijing pollution is reinforced by the AQI data for Beijing and Chengde [27]. The Chinese Government AQI is a national algorithm and cannot be meaningfully compared to other international AQIs [36].

2.4. Human Whole Blood Collection

Whole blood (10 mL) was collected using standard phlebotomy methods (WHO, 2010) and with ethical permission granted by Beijing Chao-Yang Hospital REC. Blood was drawn from the cephalic vein into a 10 mL CPT tube (Becton Dickinson, Franklin Lakes, NJ), an evacuated blood collection tube system containing sodium citrate anti-coagulant and blood separation media composed of a thixotropic polyester gel and a FICOLL™ Hypaque™ solution. Peripheral venous blood was obtained from healthy volunteers after obtaining signed, informed consent. Peripheral venous blood of 10 COPD residents in Beijing was also obtained in Beijing Chao-Yang Hospital.

2.5. Routine Blood Examination

Blood samples were collected from elbow veins of each participant in tubes containing Ethylene Diamine Tetraacetic Acid (EDTA) to measure the blood parameters (hematocrit, hemoglobin concentration, white blood cells, and heterophils) and stored at −80 °C until use.

2.6. Lung Function Test

The lung function tests were performed with Jaeger MasterScreen pulmonary function instrument (pneumotachograph; VIASIS, Würzburg, Germany) in strict accordance with the American Thoracic Society/European Society of Respiratory Diseases guidelines [37]. Each subject completed at least 3 qualified lung function measurements, and the best results were selected based on the performance of the subject and shape of the curve [38]. The subjects were sequentially examined using Impulse oscillation system (IOS), spirometric flow-volume loop measurement. Parameters of the traditional PFT recorded were as follows: forced expiratory volume in 1 s/forced vital capacity (FEV_1/FVC), FEV_1 1% predicted ($FEV_{1\%pred}$), peak expiratory flow predicted (PEF_{pred}) and maximal mid-expiratory flow predicted rates ($MEF_{75\%pred}$, $MEF_{50\%pred}$, $MEF_{25\%pred}$, and MEF_{25}/MEF_{75}). The IOS parameters recorded included total respiratory impedance [$Z_{5\%pred}$] and resistance [$R_{5\%pred}$, $R_{20\%pred}$, and $R_{35\%pred}$] parameters.

2.7. Correlation of Haematological Indices and AQI, PM10, PM2.5

To determine which haematological index responds to either AQI, PM10 or PM2.5, we calculated the correlation of each haematological index and concentration of AQI, PM10 or PM2.5 using the *cor* function in R 3.3.3. AQI, PM10 and PM2.5 data were retrieved from the website of China Air Quality Online Monitoring and Analysis Platform (https://www.aqistudy.cn/).

2.8. Isolation of Neutrophils and RNA Extraction

8 mL of blood was used for neutrophil isolation using the MACSxpress Neutrophil Isolation kit (Miltenyi, USA) following the manufacturer's protocol. RNA was extracted from the isolated neutrophils using the TRIzol™ Reagent kit (Invitrogen, UK) as per manufacturer's guidelines and then stored at −80 °C until further use.

2.9. RNA Sequencing

The RNA was purified using Dynal Oilgo (dT) beads (Invitrogen) and then fragmented into 350 bp fragments using RNA Fragmentation Reagents (Ambion), followed by cDNA synthesis using random primers (Invitrogen), Superscript II (Invitrogen), RNase H and DNA polymerase I, and further end-repair with Klenow polymerase, T4 DNA polymerase and T4 polynucleotide kinase (for blunt-ends of DNA fragments; Invitrogen). cDNA libraries were constructed following the manufacturer's protocol (Illumina) and subjected to sequencing on a Hiseq2500 platform (Illumina) at Novogene. Raw data were filtered by removing adaptors and reads with unknown nucleotides more frequent than 10% as well as those with low quality (where PHRED values were less than 10 for more than 50% of the bases).

2.10. Transcript Quantification

Approximately 5 Gb cleaned data across 30 samples were aligned to the human reference genome (GRCh38), combined with the known gene annotation (Ensembl87), using improved version HISAT2 v.2.0.1 with parameters -N 0, -I 100, -X 600, -fr, -tmo [39]. Stringtie v.1.2.0 [40] was used with default parameters to reconstruct transcript annotations across the genome merged with reference gene model. The expression of each transcript was quantified as *TMP* using RSEM [41] and required $TPM \geq 1$ to be considered.

2.11. Correlation between Transcript Expression and PM2.5, PM10, AQI

For each expressed transcript, the correlations between its expression level and either PM2.5, PM10, or AQI concentration were calculated using the *cor* function implemented in R 3.3.3. PM2.5, PM10 and AQI were retrieved from the website of China Air Quality Online Monitoring and Analysis Platform (https://www.aqistudy.cn/).

2.12. ESE Identification

We first classified the AS-derived transcripts into three datasets: 1) expressed in all BRs but none in CRs, referring as BR specific transcripts; 2) expressed in all CRs but none in BRs (CR specific transcripts); 3) expressed in all recruits (BR-CR shared transcripts). For each dataset, we randomly chose 100 transcripts for ESE identification using ESEfinder 3.0, a web-based software [42], followed by calculating the frequency of each ESE. It is noted that CR specific transcripts were excluded for ESE identification because only seven transcripts were identified.

2.13. DET (Differentially Expressed Transcript) Identification

We used four methods to identify DETs between the Beijing and Chengde populaces due to the large amount of biological variation between the individuals sampled. In this respect, to obtain a DET set with high reliability, we applied multiple tests to highlight only the most supported DETs [43]: edgeR-robust [44] and DESeq 2 [45] based on exact

tests, a non-parametric test in SAMseq [46], and an empirical Bayesian analysis using Limma [47]. A total of 5,397 robust DETs were supported by all four methods and were used in downstream analysis. KEGG enrichments for down-regulated DETs were conducted using a hypergeometric test.

2.14. Variance Analysis of Physiological Phenotypes

To identify the isoform of which the expression was significantly correlated with a physiological phenotype of interest, we conducted Analysis of Variance (ANOVA) with each haematological index as the dependent variable and expression of isoforms as the independent variables, using the *ano* function implemented in R3.3.3.

2.15. Cytokine ELISA

The relative concentration of plasma cytokine expression was measured by ELISA using the Human ICAM-1/CD54, IL-8/CXCL8, MIF, IL-6 and C-Reactive Protein/CRP via the Quantikine ELISA Human (R&D Systems, UK). Kits were used according to manufacturer's instructions. Briefly, plates were coated with monoclonal anti-human cytokine capture antibody and blocked with 1% bovine serum albumin. Plasma samples, in triplicate, were incubated for two hours at room temperature together with recombinant human cytokine standards. Bound cytokine was detected with anti-human cytokine horseradish peroxidase secondary antibody and tetramethylbenzidine substrate. The concentration of cytokine per sample was calculated using a four-parameter logistic curve fit of the standard concentrations. All data were expressed as mean ± S.D. and for comparisons of the means, the student t-test was used. *P* values less than 0.05 were considered statistically significant.

2.16. Cytokine Array

The relative concentration of plasma cytokine protein concentration was determined by cytokine array was assessed using the Proteome Profiler Human Cytokine Array (Panel A Kit, R&D Systems, Minneapolis, USA). Arrays were used according to manufacturer's instructions. Briefly, plasma was incubated with nitrocellulose membrane coated with 36 different capture antibodies. Bound cytokines were detected with a cocktail of secondary biotinylated antibodies and streptavidin-HRP. Membranes were imaged using ChemiDocTMXRS + System (BioRad). ImageJ software (Version 1.5.1,2018) was used to determine the average pixel density of the duplicate spots.

3. Results

3.1. Selecting Beijing and Chengde as Investigation Sites

An ideal comparative study is to investigate a location with well-recognized AP problems, and a comparison site with AP of similar provenance and composition, but at significantly lower levels. The megacity of Beijing was selected given that the city suffers from some of the worst AP Worldwide. Beijing's widespread AP can be attributed to **anthropogenic, technogenic and geogenic factors including** a **surge in the number of motorized vehicles**, **population growth output from manufacturing** and **contributions from natural PM sources, such as the city's surrounding topography and seasonal weather.** Our previous research [28-35] on the physiochemical characteristics of Beijing AP, specifically the PM component, confirmed via electron microscopy, the presence of combustion-derived PM dominated by DE from vehicles, CB from cooking and FA from heating activities. In addition, there are platy minerals originating from the local geology of Beijing due to its proximity to the Gobi Desert, as well as fugitive dust from its satellite cities.

Monitoring of Beijing's wind directions illustrated a clear annual pattern along a northeast-southwest (NE-SW) transept (**Figure 1**). Located to the south of Beijing are sev-

eral industrialized satellite cities generating AP with clear coal-burning and steel manufacturing characteristics (e.g. FA and smelter particles) (**Table S1**). Therefore, these cities are unsuitable for comparison with Beijing. Chengde, located 110 miles NE of Beijing, on the contrary, is a small city that is not as industrialized as the satellite cities to the south and it is along the recognized 'NE-SW AP transport corridor' (**Figure 1**). Therefore, it is expected that the lower degree of industrialization, along with the NE-SW wind direction transept, renders Chengde having the PM provenance and composition like Beijing, but at significantly lower levels.

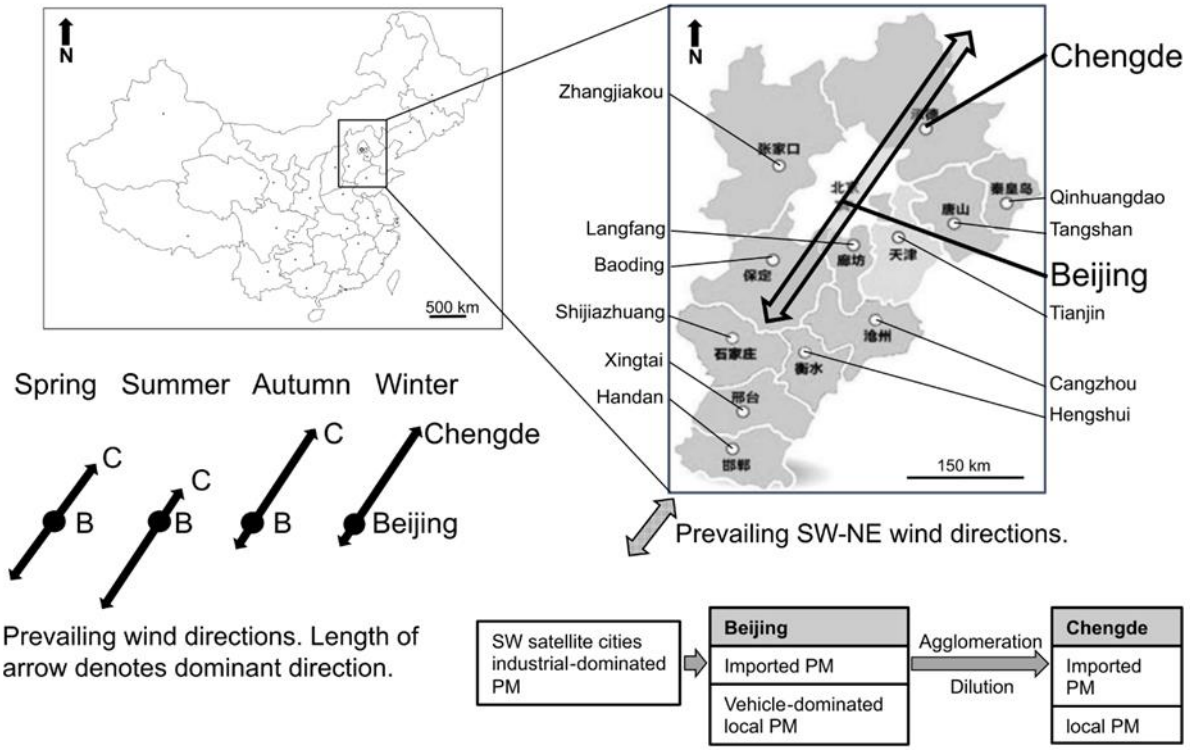

Figure 1. Geographical locations of Beijing and the satellite cities, featuring Chengde and the NE-SW AP transport corridor. In spring, the wind blows equally to the NE and SW, in summer it is mostly winds to the SW. However, in the autumn and winter, which is the most heavily polluted time of the year, the predominate wind direction is from Beijing to Chengde [27].

Indeed, considering the role of particle physiochemistry and toxicological effects, the daily air quality data of Beijing and Chengde, derived from the Chinese Government AQI website (https://www.aqistudy.cn/) revealed: (1) Beijing has a consistently higher AQI compared to Chengde; (2) Beijing has a consistently higher PM2.5 component than Chengde; (3) the mass concentration of PM10 in Beijing is consistently higher than Chengde and the chemical composition of their respective airborne pollutants is not dissimilar due to a shared source apportionment (i.e. traffic emissions, steel production and fugitive mineral dusts) via the seasonal wind transepts; (4) Chengde has relatively higher SO_2, but the actual levels are low. The relatively higher SO_2 in Chengde may represent its local industry or other sources (**Table S2**).

To determine how long Beijing AP would take to arrive at Chengde, we conducted linear regression analyses on both data. The linear regression line for X (Beijing)-Y (Chengde) for the same day has a $R^2 = 0.0958$. A one-day lag into the data X (Beijing + one day)-Y (Chengde), on the assumption a pollution peak in Beijing should reach Chengde the next day, achieved an improved $R^2 = 0.1172$. A two-day lag provided a lower $R^2 = 0.00763$ and a three-day lag resulted in an even lower $R^2 = 0.00556$. These results suggested that Chengde AP had a one-day lag-time from Beijing pollution; consistent with a recent

report [27]. These conclusions enabled us to qualify Chengde as an ideal comparison site with Beijing in our study.

3.2. Physiological Responses upon PM Exposure and Data Generation

In order to reduce confounding factors, 10 healthy (i.e., non-smokers with no pre-existing cardio-pulmonary disease) recruits with ages ranging from 23 to 39 from each city (**Table 1**) were selected. Peripheral venous blood for routine blood examination was obtained from each volunteer followed by lung function tests. In addition, 10 COPD patients from Beijing were recruited (**Table 2**) and routine blood examinations and lung function tests were conducted. Finally, specific soluble inflammatory mediators were measured using ELISA to help identify the genes and gene networks differentially activated in response to these exposures.

Table 1 Information for healthy recruits from Beijing and Chengde.

City	Sample ID	Sex	Sample type	Age (yr)	Height (cm)	Weight (kg)
Chengde	201705CD0001	Female	RNA+plasma	23	163	52
	201705CD0002	Female	RNA+plasma	29	169	52
	201705CD0003	Female	RNA+plasma	26	168	48
	201705CD0004	Female	RNA+plasma	25	160	50
	201705CD0005	Female	RNA+plasma	25	159	55
	201705CD0006	Male	RNA+plasma	26	170	53
	201705CD0007	Male	RNA+plasma	28	175	90
	201705CD0008	Male	RNA+plasma	26	178	100
	201705CD0009	Male	RNA+plasma	31	173	81
	201705CD0010	Male	RNA+plasma	30	183	80
Beijing	201705IOZ0001	Female	RNA+plasma	26	173	65
	201705IOZ0002	Female	RNA+plasma	24	167	60
	201603IOZ0014	Male	RNA+plasma	22	178	82
	201603IOZ0011	Male	RNA+plasma	29	167	63
	201603IOZ0002	Female	RNA+plasma	25	160	50
	201603IOZ0009	Male	RNA+plasma	33	160	58
	201603IOZ0012	Male	RNA+plasma	27	176	80
	201603IOZ0006	Male	RNA+plasma	38	169	67
	201703IOZ0013	Male	RNA+plasma	27	180	65
	201711IOZ0012	Male	RNA+plasma	39	178	78

Table 2 Information for 10 COPD participants from Beijing.

City	Sample ID	Sex	Sample type	Age (yr)	Height (cm)	Weight (kg)
Beijing	201612cy0001	Male	RNA+plasma	58	168	78
	201612cy0002	Male	RNA+plasma	58	165	46
	201612cy0003	Male	RNA+plasma	70	160	57
	201612cy0004	Male	RNA+plasma	60	165	61
	201703cy0006	Male	RNA+plasma	56	160	58
	201703cy0007	Male	RNA+plasma	56	161	61
	201703cy0008	Male	RNA+plasma	82	163	61
	201703cy0009	Male	RNA+plasma	64	157	50
	201711cy0010	Male	RNA+plasma	67	172	88
	201711cy0011	Male	RNA+plasma	77	165	48

A comparison of lung function tests (FEV_1/FVC; **Figure 2a**) between BRs (81 ± 5) and CRs (90 ± 9) as well as COPD (47 ± 16) patients demonstrated there was a statistically significant decrease of lung function ($P < 0.01$, t-test) in the BRs compared with CRs, but not severe since non-significance for $FEV_1pred\%$ (93 ± 12 in BRs *vs*. 93 ± 11 in CRs; $P = 0.97$, t-test). Lung function was further decreased and exacerbated in COPD recruits ($FEV_1pred\%$:40 ± 20; $P < 0.001$ for both FEV_1/FVC and $FEV_1pred\%$, t-test), suggesting that inflammation responses have been induced in both BRs and COPD groups.

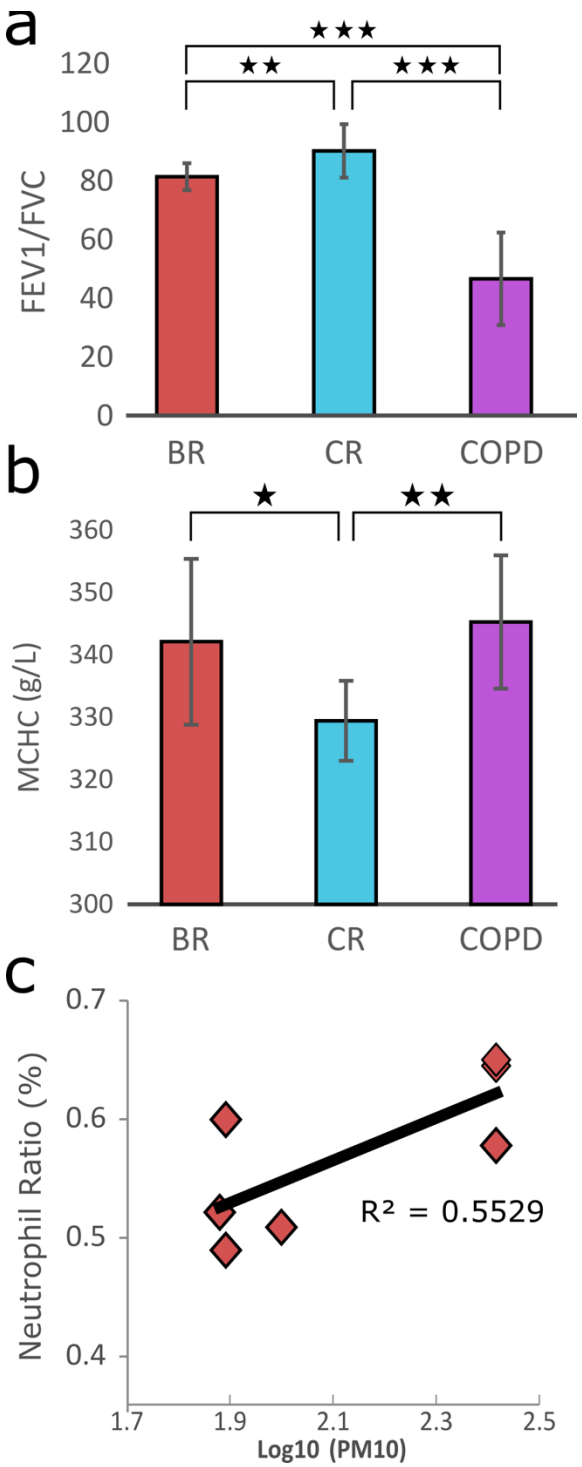

Figure 2. Physiological responses upon AP exposure. (**a**) Comparison of lung function indexed by FEV1/FVC between BRs, CRs and COPD patients. (**b**) Comparison of mean corpuscular haemoglobin concentration between BRs, CRs and COPD patients. (**c**) Correlation between PM10 and ratio of neutrophil. Error bars indicate standard error of mean (SEM). * $P < 0.05$, ** $P < 0.01$, *** $P < 0.001$, t-test.

Among a total of 16 haematological indices that were examined in the routine blood examinations, MCHC (mean corpuscular haemoglobin concentration) revealed a significant difference among the three groups, with higher MCHC (**Figure 2b**; 342 ± 13 in BRs *vs.* 329 ± 4 in CRs, $P = 4.38E\text{-}6$, t-test) in BRs and even higher MCHC in COPD volunteers (348 ± 8); collectively indicative of hypoxia induction in both BRs and COPD participants. Notably, the lack of statistically significant difference in other indices (e.g. neutrophils,

RBCs, haemoglobin, monocyte and macrophage, *etc.*) between CRs and BRs (but not between CRs or BRs and COPD group; **Figure S1**) suggested that stress induced by PM exposure has been well handled in BRs.

To determine which haematological indicator played the most important role in reacting to PM among these examined indices, we carried out correlation analyses for each index against PM10 concentration, respectively, and found that neutrophil ratio had the largest correlation coefficient (R^2 = 0.55, **Figures 2c** and **S2**). Hence, we first sequenced the transcriptomes of neutrophils in both BRs and CRs and conducted comparative transcriptomic analysis to provide insight into the mechanisms underlying how PM-induced stress had been so well addressed.

3.3. Alternative Splicing in BRs and CRs

RNA extracted from neutrophils of each volunteer (N = 10) was subjected for sequencing on an Illumina X-Ten sequencer, yielding about 5 gigabases (Gb) of clean RNA-seq data for each sample. Cleaned reads for each sample were aligned to the GRCh38 human reference genome using HISAT [39]. The expression of each transcript was quantified as transcripts per million (TPM) using RSEM [41]. On average, BRs expressed over 36,000 (36,274 ± 1389) transcripts, significantly higher than Chengde (24,160 ± 1919) (**Figure 3a**, $P < 0.001$, t-test). Two possible factors may lead to this scenario: (1) more gene loci were expressed in BRs and, (2) AS occurred more frequently in BRs. Our analyses revealed that BRs expressed, on average, 1000 gene loci more than CRs, yielding ~2000 transcripts, contributing only 18% of the increased transcript number (~12,000) in BR. Strikingly, we found that 6760 of the gene loci expressed in both groups generated significantly more isoforms in BRs compared with CRs (**Figure 3b**, $P < 0.05$ for each gene locus, t-test), resulting in an increment of approximately 10,000 transcripts. This accounted for 80% of the 12,000 transcripts uniquely expressed in BRs, suggesting that 'alternative splicing' serves as a major source in generating such a large abundance of transcripts, thus setting the scene for the development of biological 'resilience'.

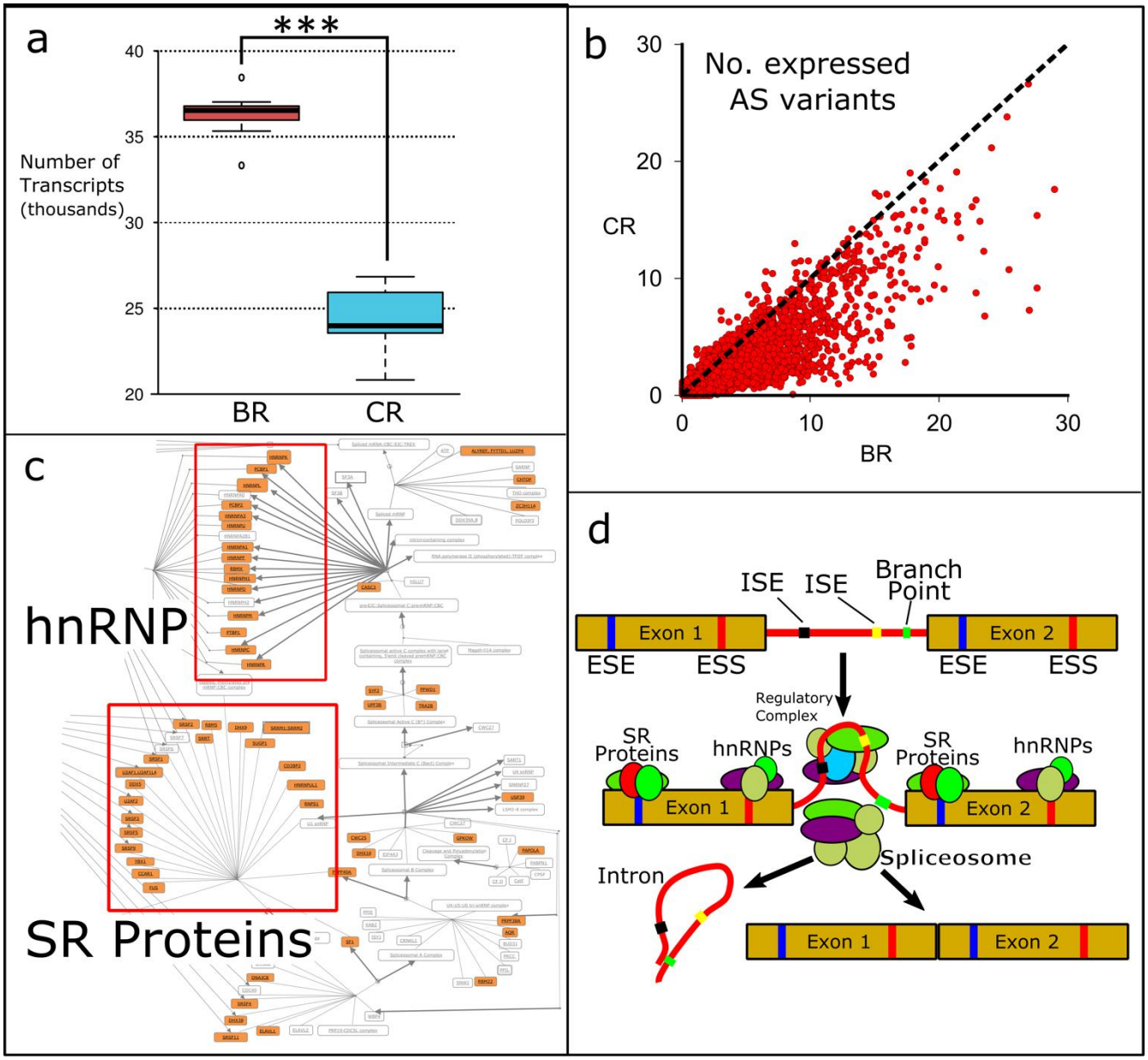

Figure 3. Alternative splicing is the major factor generating large abundance of transcripts during AP exposure. (**a**) The number of expressed transcripts in BRs and CRs. Error bars indicate standard error of mean (SEM). *** $P < 0.001$, t-test. (**b**) The number of expressed AS-derived transcripts for each of the 6760 genes in BRs (x-axis) is plotted against that in CRs (y-axis). (**c**) Genes generating more AS-transcripts in BRs in the major mRNA splicing pathway were denoted as orange. Red box indicated hnRNP and SR protein families. The pathway is modified from http://www.reactome.org/content/detail/R-HSA-72163. (**d**) A schematic graph showing how hnRNP and SR proteins cooperate during pre-mRNA splicing. This model is modified from a previous study [48].

We next carried out functional enrichment analysis on the 6760 genes. Interestingly, the results showed that the most significant enriched item referred to RNA splicing (**Table S3**). Therefore, we focused on the AS patterns in the RNA splicing major pathway. Our analysis revealed that AS events occurred dominantly in gene families encoding hnRNP (heterogeneous ribonucleoproteins) and serine/arginine (SR)-rich proteins; the master regulators in alternative splicing (**Figure 3c**) [49-51]. The occurrence of RNA splicing relies on the concerted roles of both SR and hnRNP with the former mainly binding to ESE (exonic splicing enhancer) element and the latter to ESS (exonic splicing silencer) in exons to recruit the slicing complex to the targeted splicing site (**Figure 3d**) [49-51]. Given that different SR and hnRNP isoforms bind to different ESEs and ESSs [52], the AS of SR and

hnRNP gene families may constitute a 'molecular basis' of the unexpected large number of isoforms in Beijing participants because abundant SR and hnRNP isoforms generated will enlarge the reservoir of ESEs and ESSs that could be bound.

To determine whether these AS-derived transcripts have any protective roles against PM exposure, we first calculated the correlation between the expression of each AS-derived transcript and AQI, PM2.5 or PM10 concentrations, then classified these AS-derived transcripts as BR-specific, CR-specific and BR-CR shared transcripts and finally estimated their proportions of transcripts, whose expression was significantly correlated with either of these indices. We found that 30% of BR specific transcripts were significantly correlated with either PM2.5, PM10 or AQI, much higher than either CR specific (18%) or shared transcripts (7%; **Figure 4a**). Among the 100 AS-derived transcripts showing the most significant correlation with AQI, PM2.5 or PM10, over 70% belong to BR specific transcripts (**Figure 4a**).

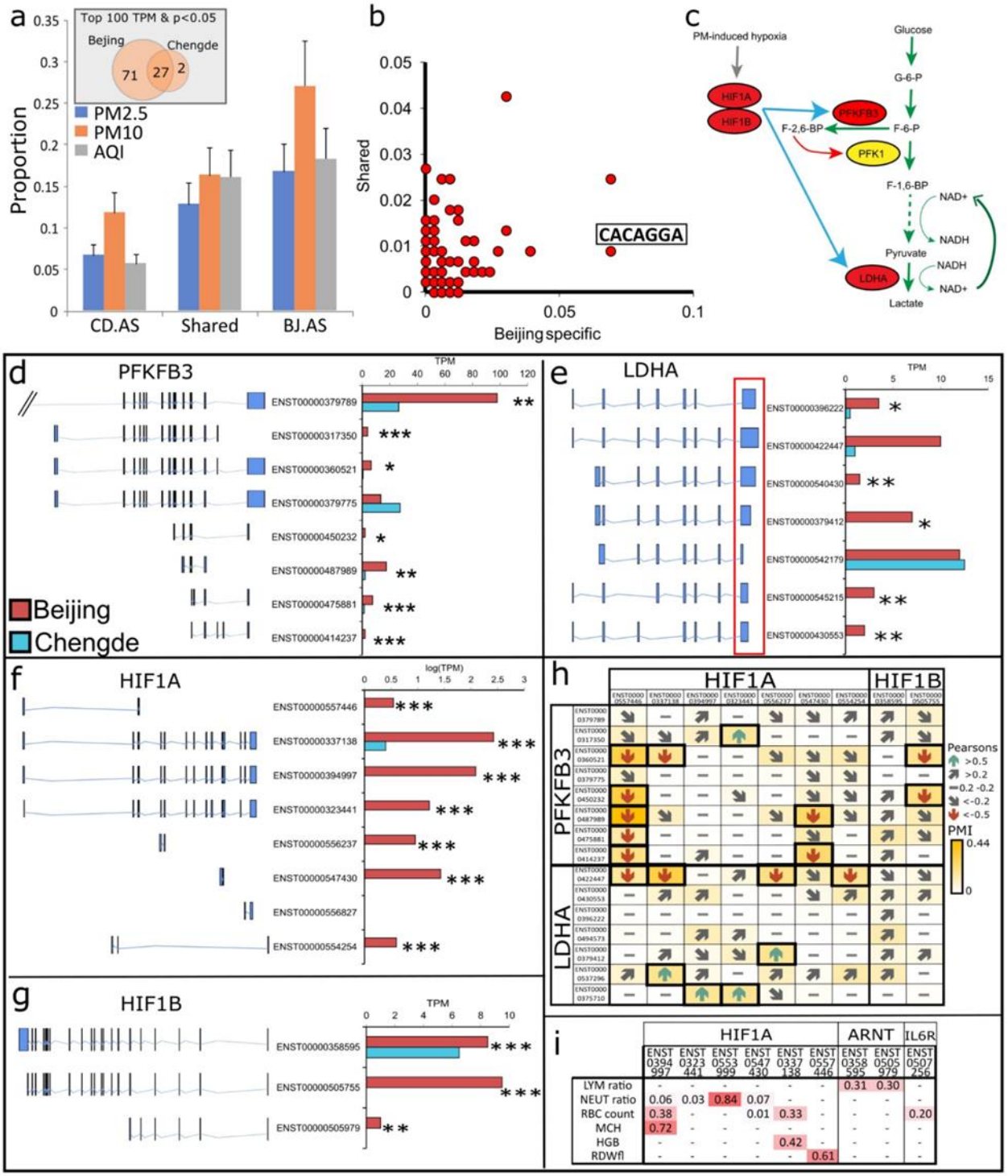

Figure 4. Roles of alternative splicing in responding to AP exposure. (**a**) Proportions of AS-derived transcripts, whose expression is significantly correlated with either AQI, PM10 and PM2.5, for BR-specific, CR-specific and BR-CR shared AS-derived transcripts. CD.AS: CR-specific AS-derived transcripts; Shared: BR-CR shared AS-derived transcripts; BJ.AS: BR-specific AS-derived transcripts. The sub-figure on the top left showed the classification (BR-specific, Shared and CR-specific) of the top 100 AS-derived transcripts showing the most significant correlation with either AQI, PM2.5 and PM10. (**b**) Utilization frequency of each ESE element between BR-specific and shared transcripts with one element *CACAGGA* being highlighted. *X*-axis represents the observed frequency for BR-specific AS-derived transcripts and *y*-axis is the frequency for shared AS-derived transcripts. (**c**) A pathway showing the roles of HIF1A, HIF1B, PFKFB3, PFK1 and LDHA in glycolysis. (**d-g**) Alternative splicing patterns of *PFKFB3*, *LDHA*, *HIF1A* and *HIF1B* with expression of each isoform in BR and CR shown in the right. * $P < 0.05$, ** $P < 0.01$, *** $P < 0.001$, t-test. (**h**) Pearson correlation and PMI between expression of each *PFKFB3*, *LDHA* isoform and that of each *HIF1A*, *HIF1B* isoform. (**i**) Variance explanation of each isoform of *HIF1A*,

HIF1B (also referred as *ARNT*) and *IL6R* for each physiological index. The redder the color is, the more variance it could be explained.

We further compared the utilization frequency of each ESE element between BR-specific and shared transcripts and showed that the utilization frequencies of several ESEs significantly differ between the two groups, exemplified by one ESE element (i.e., *CACAGGA*) exhibiting six times of its frequency higher in the former (7%) than that in the latter (1%) (**Figure 4b**). Transcripts containing *CACAGGA* are significantly enriched in C2H2 type zinc finger gene families, which have been implicated in regulating immune responses through mediating IL and INF pathways, and oxidative responses to biotic and abiotic (i.e., ambient particulate matter) [53, 54]. Overall, our results implied that AS indeed has potential protective roles in abrogating exposures to poor air quality. We next sought to know which roles of AS acts as in addressing PM exposure.

3.4. AS Reshapes Glycolysis Landscape

The higher MCHC observed in BRs (**Figure 2b**) in our study suggested that hypoxia, a hallmark of long-term exposure to poor air quality [55], has been induced. Upon hypoxia, neutrophils would be activated and utilizing ATP mainly generated through glycolysis [56, 57], and it has been documented that glycolysis was enhanced when exposed to PM [58, 59]. However, there is a paucity of information about how this enhancement is achieved. To address this issue, we investigated the AS patterns of all genes ($N = 12$) which encoded essential enzymes in the glycolysis pathway and found that two exhibited distinct AS patterns between CRs and BRs (i.e. *PFKFB3* (*6-Phosphofructo-2-Kinase/Fructose-2,6-Biphosphatase 3*) and *LDH* (*Lactate dehydrogenase*)).

PFKFB3 encodes an enzyme that has been reported to have the highest kinase activity to shunt glucose toward glycolysis [60]. It converts fructose-6-phosphate to fructose-2,6-bisP (F-2,6-bisP), which allosterically activates PFK-1 (6-phosphofructokinase-1), the rate-limiting enzyme in glycolysis [48]. The activated PFK-1 acts as a key player in stimulating glycolysis under hypoxia (**Figure 4c**) [48]. We found that BRs expressed eight *PFKFB3* isoforms, compared with only three in CRs (**Figure 4d**). Expression levels of four isoforms were significantly correlated with PM concentration (**Figure S3**). Further analyses showed that these four isoforms were resulted from AS of exons encoding COOH-terminal, leading to different COOH-terminal regulatory domains. Since different COOH-terminals result in differential localization of PFKFB3 protein to different sub-cellular compartments (e.g., cytoplasm, peroxisome, nucleus) [60]; we suggest that AS of *PFKFB3* may play an important role in stimulating glycolysis upon PM exposure. Additionally, among these isoforms exclusively expressed in BRs, one isoform (ENST00000360521, *UBI2K4*), possessing a COOH-terminal with higher kinase activity than other isoforms [61], has been suggested to be induced by hypoxia [61, 62]. The induced expression of this isoform may be expected to enhance glycolysis.

LDHA encodes lactate dehydrogenase A (LDHA), catalyzing the conversion of pyruvate and NADH to lactate and NAD^+, with NAD^+ being a pre-requisite driver for glycolysis [63]. We found that the number of seven *LDHA* isoforms were expressed in BRs, in contrast with only three in CRs (**Figure 4e**), leading to a total of *LDHA* expression in BRs being six times higher than that in CRs (*TPM* = 603 in BRs *vs.* 93 in CRs). The expression levels of two isoforms (*LDHA-005*: *ENST00000379412* and *LDHA-001*: *ENST00000422447*) exhibited significant correlation with PM concentration (**Figure S4**). Interestingly, these two isoforms share exactly the same open reading frame (ORF) with the one dominantly expressed in CRs (*LDHA-020: ENST00000542179*), with the major difference being that both isoforms (*LDHA-005* and *LDHA-001*) feature much longer 3'UTR lengths (i.e. 566 and 1144bp longer than *LDHA*-020). Since longer 3'UTR can enhance both mRNA stability and translational efficiency [64], it is expected that BRs may generate more LDHA proteins, which may in turn promote the formation of NAD^+, allowing the enhancement and maintenance of glycolysis.

Pyruvate could be converted either to lactate for NAD^+ generation or to acetyl-CoA, which could finally enter the electron transport chain (i.e. oxidative phosphorylation; OP) for ATP generation. Since *LDHA* was over-expressed in BRs, it is expected that a large proportion of pyruvate would be catalyzed to lactate rather than acetyl-CoA. Given that glucose serves as a major energy source in neutrophils [19], we expected that OP would be downregulated in BRs. Consistently, functional enrichment analyses on transcripts significantly downregulated in BRs showed that the most significantly enriched KEGG pathway was OP (**Figure S5**). OP is a process by which electrons are transferred to O_2 molecules through respiratory complexes to generate ATP. Once there are insufficient O_2 molecules to accept electrons, electrons would leak out of the electron transfer chain to generate toxic reactive oxygen species (ROS) [65], which would induce cell and macromolecule (i.e., DNA, RNA, and proteins) damages [66]. Therefore, OP reductions in BRs would act to minimize the generation of toxic ROS under hypoxic conditions.

Next, we were interested to know how the two genes were regulated upon polluted air exposure. A survey on published literature identified one common transcription factor, hypoxia-inducible factor 1 (HIF-1) [67, 68]. HIF-1, a master regulator of oxygen homeostasis, consists of two sub-units: an inducibly expressed HIF-1A and a constitutively expressed HIF-1B [69]. We therefore investigated the AS patterns of these two genes. In our study, CRs expressed only one *HIF-1A* and one *HIF-1B* isoforms, in sharp contrast with seven and three isoforms in BRs (**Figures 4f** and **4g**). A co-expression analysis showed that different isoforms of *HIF-1A* and/or *HIF-1B* were significantly co-expressed with different isoforms of *PFKFB3* and *LDH* (**Figure 4h**). To investigate whether these observed associations are direct, we applied a recently developed algorithm based on information theory, which was reported to accurately quantify direct relations between measured variables with higher statistical power by silencing indirect effects [70]. The results showed that different *HIF-1A* and/or *HIF-1B* isoforms can directly regulate the transcription of distinct *PFKFB3* and *LDH* isoforms (**Figure 4h**).

Taken together, we concluded that chronic exposure of PM air pollution imposes hypoxic stress, promoting AS of *HIF-1A* and *HIF-1B*, which further induces the AS of *PFKFB3* and *LDHA*. The resultant AS of *PFKFB3* and *LDHA*, collectively, may modulate glycolysis in neutrophils in that: (1) AS of *PFKFB3* led to PM-associated isoforms (PMAI) with different COOH-terminal regulatory domains, which may target different sub-cellular locations, and consequently, stimulate glycolysis; (2) AS of LDHA gave rise to two PMAIs with longer 3'UTRs relative to the constitutively expressed one, possibly enhancing mRNA stability and translational efficiency, and thus, promoting LDHA generation and subsequently glycolysis enhancement and maintenance.

Given that HIF-1 is the key regulator of hypoxia response [69], the observation that a total of 10 *HIF-1* isoforms (7 *HIF-1A* and 3 *HIF-1B*; **Figures 4f** and **4g**) were expressed in BRs, raises one essential question: *Whether these isoforms played the same or diverse roles upon PM-induced hypoxic conditions?* To address this issue, we estimated the associations between the expression of these isoforms and different hypoxia-associated physiological responses (e.g. RBC count, MCH, hemoglobin count, RBC volume distribution width (RDW), neutrophil count and neutrophil ratio). Strikingly, our results revealed that different isoforms show significant correlation with varied physiological indices (**Figure 4i** and **Table S4**). For instance, expression of *HIF1A-003* (*ENST00000394997*), *HIF1A-005* (*ENST00000553999*), *HIF1A-001* (*ENST00000337138*) and *HIF1A-008* (*ENST00000557446*) could explain 72%, 84%, 42% and 61% variances of MCHC, neutrophil ratio (i.e., the ratio of neutrophils among whole blood cells), hemoglobin count and RDW (red cell distribution width) **(Figure 4i** and **Table S4**; all $P < 0.05$). These findings highlighted that different isoforms may have diverse physiological functions.

3.5. AS Prolongs Neutrophil Lifespan and Enhances Migration in BRs

It has been recognized that upon immune response, neutrophils would extend their lifespan from 6-12 to 24-72 hours primarily by mitigating apoptosis [71]. During this process, two distinct signalling pathways (i.e., intrinsic and extrinsic) have been proposed with the intrinsic pathway mediated by anti-apoptotic protein Mcl-1 and the extrinsic pathway mediated by death receptors such as Fas (a cell surface death receptor), TNF-related apoptosis-inducing ligand receptors and TNF receptors [72]. AS analyses of these genes showed that only *Fas* underwent AS, leading to 9 isoforms with either exon 6 or 9 truncated and 7 were exclusively expressed in BRs, accounting for ~70% of the expression in this locus that sharply reduced the expression ratio of intact *Fas* to 30%, which is, however, significantly lower than that in CRs (90%; **Figure S6**).

Fas is a transmembrane protein, encoded by a nine-exon gene, with the 6th exon encoding a transmembrane domain and the 9th encoding a death domain (DD), both of which are critical for the transmission of an apoptotic signal[65]. Generally, three Fas proteins form a trimer on the membrane. Only a trimer composed of three intact Fas proteins can successfully transmit the apoptotic signals when binding with its ligand (Fas-L) [73]. In our case, we found that BRs increased the expression of truncated *Fas* isoforms lacking either transmembrane or DD domains, leading to a sharp reduction of the expression ratio of intact *Fas* (30% vs. 90%; **Figure S6**). It is expected that the increase of these truncated isoforms will compete with intact Fas to form non-functional trimers, thereby inhibiting apoptosis. Consistently, the expression of these truncated Fas isoforms could respectively interpret 81%, 86%, 77% and 67% variances of the counts of WBC, neutrophils, and lymphocytes as well as lymphocyte ratio in the Beijing population of recruits (**Figure S7** and **Table S5**). Altogether, we proposed that the induction of these AS-derived truncated *Fas* isoforms serves as a means to effectively inhibit apoptotic signal transmission in neutrophils, thus prolonging their lifespan when exposed to poor air quality.

Previous studies suggested that neutrophils would enhance their migration capacity because of immune responses [74]. Expectedly, MIF, a marker indicating cell migration capacity [75-78], was upregulated in BRs determined by ELISA, indicative of enhanced migration ability (**Figure S8**). To obtain insight into the molecular basis of neutrophil migration capacity enhancement in BRs, we determined the levels of an array of cytokines that could promote neutrophil migration in both BRs and CRs. IL-6, one cytokine that has been well established in promoting neutrophil migration [79], was over-expressed in BRs. IL-6 can bind either to the membrane-bound IL-6R mediating the classic signaling mode, or to the soluble IL-6R without the transmembrane domain, triggering a trans-signaling mode [80]. CRs were found to express only membrane-bound *IL-6R* isoform, which was significantly upregulated in BRs (**Figure S9**). Moreover, BRs expressed an extra of six isoforms without the transmembrane domain (**Figure S9**), the expression of which was significantly correlated with the neutrophil ratio (**Figure S10**), implying that BR neutrophils might adopt both IL-6 signaling modes for migration. Given that cells using both IL-6 signaling modes have higher migration capacity than the ones owning only one [81], we concluded that featuring two modes of IL-6 signaling along with the up-regulation of IL-6, enables BR neutrophils to enhance their migration ability. Altogether, AS of *IL-6R* provides a means to enhance the neutrophil migration for individuals exposed to polluted air.

3.6. HIF-1 Mediated Impaired Glycolysis Mediates Neutrophil Dysfunction

Dysfunction in activated neutrophils, when exposed to PM have been implicated in promoting pathogenesis of a number of human diseases, such as COPD, due to their impaired immune functions (e.g., impaired phagocytosis [82], reducing capacity of pathogen killing [83] and clearance [84] and reduction of chemotactic accuracy [85]). However, knowledge of the molecular basis mediating these impaired immune functions in neutrophils remains largely unexplored. A comparison between the transcriptome profiles of BRs and COPD volunteers in Beijing may provide some clues to this question.

Our results showed that neutrophils isolated from COPD patients have comparative number of expressed transcripts with that from BRs (34,233 ± 3459 in COPD *vs.* 36,274 ± 1389 in BRs, $P = 0.13$), and share similar AS patterns of both *Fas* and *IL-6R*. However, *HIF1A* and *PFKFB3* exhibited distinct AS patterns between the two groups. For instance, only 5 *HIF1A* isoforms were expressed in COPD patients, in contrast with 7 in BRs, giving rise to reduced expression of this gene loci (*TPM* = 132 in COPD patients *vs.* 413 in BRs). Consistently, isoform numbers of *PFKFB3* have also been reduced in COPD patients relative to BRs (4 in COPD and 8 in BR). Unexpectedly, expression analyses showed that, when compared with CRs, there were no statistically significant expression difference for *PFKFB3* (*TPM* = 83 ± 62 in COPD *vs.* 77 ± 55 in CRs, $P > 0.05$), implicating impaired glycolysis in neutrophils of COPD patients. Interestingly, when we plotted their expression or isoform numbers against the lung function (FEV_1/FVC) of CR, BR and COPD patients (**Figure S11**), a reverse "U" (referred as "∩" hereafter) pattern was observed for the two genes (i.e. *HIF1A*, *PFKFB3*). That is, the initial lung function reduction was accompanied with the up-regulation and increased isoform number of the focal genes (from CRs to BRs), followed by subsequent down-regulation and isoform number decrease upon further lung function reduction (from BRs to COPD patients; **Figure S11**).

Given that immune functions (e.g. phagocytosis, degranulation, *etc.*) of neutrophils rely on ATP dominantly generated from glycolysis [19], impaired glycolysis may lead to dysfunctions of neutrophils [19]. In our case, we proposed that the reduction of *HIF-1A* expression and AS-derived isoform number mediates the impaired glycolysis through down-regulating the expression of the key enzyme encoding gene (i.e. *PFKFB3*), and reducing its AS. Therefore, *HIF-1A* and *PFKFB3* may act as key players mediating dysfunction of activated neutrophils and serve as an essential biomarker in monitoring neutrophil function.

4. Discussion

Our study and others [86, 87] have implicated that neutrophils act as the key player in response to poor air quality. It is further demonstrated that dysfunction of neutrophils plays a critical role in pathogenesis progression when long-term exposed to polluted air [19, 88]. To our knowledge, our study, based on a hierarchical design of comparative toxico-transcriptomes, represents the first attempt to characterise the molecular mechanisms underlying how neutrophils properly buffer the stresses imposed by long-term exposure of urban PM and how their immune functions become impaired in 'real-life' settings.

In our investigation, we demonstrate that AS may promote the expression of different *PFBFK3* isoforms targeting distinct sub-cellular locations, and thus, stimulating glycolysis regionally. Given that different sub-cellular compartments are responsible for distinct immune functions [89], and these functions mainly rely on ATP generated from glycolysis in neutrophils, the induction of these different *PFBFK3* isoforms provides molecular evidence in understanding how neutrophils trigger different immune functions subcellularly upon exposure to poor air quality. AS also leads to the expression of *LDHA* isoforms with longer 3'UTRs, likely enhancing the mRNA stability and translation rate, which is expected to facilitate generation of NAD+, a pre-requisite driver for glycolysis, hence maintaining glycolysis. In addition, AS promotes the expression of non-functional *Fas* isoforms, resulting in the reduction of intact *Fas* proportion, which is expected to inhibit the transmission of apoptotic signals and prolong the neutrophil lifespan. Moreover, AS allows BRs to feature both membrane-bound and soluble *IL-6R* isoforms, which may enhance the migration capacity of neutrophils. These functional roles of AS, however, cannot be achieved through expression regulation (i.e. up-regulation or down-regulation). Therefore, we believe that AS in neutrophils provides an irreplaceable means of regulating 'environmental fitness' or 'resilience' in the face of continuous inhalation exposure challenges to poor air quality.

It has been suggested that the characterization of neutrophil metabolic shift has currently become an emerging and active field that may provide essential knowledge on neutrophil physiology and pathology [19] regarding its role in inflammation response and pathogenesis progression. The link between metabolic shift and neutrophil inflammation response and pathogenesis progression has been outlined in many studies [90-92]. However, the molecular basis underlying metabolic shift has not yet been explored. Given that hypoxia is a key factor mediating metabolic shift during the inflammatory response and neutrophil dysfunction, the characterization of "∩" patterns of expression and isoform diversity of *HIF-1A*, a key modulator of hypoxic stress, may represent a common feature of neutrophils underpinning the transition of metabolism occurring from the beginning of neutrophil activation to normal immune function response, and further to neutrophil dysfunction and the subsequent disease progression. These "∩" patterns may also provide some hints for understanding the molecular mechanism underlying impaired glycolysis in other organs (e.g., liver [93]) upon PM exposure.

During air pollution exposure, neutrophils act as a key player mediating crosstalk among other cell types to promote inflammatory responses [20-22]. The consequences of such crosstalk could be reflected as physiological phenotypes measured by different haematological indices (e.g. RBC and WBC counts, MCHC, *etc*.) and protein. However, the molecular evidence linking air pollution exposure and these physiological phenotypes in neutrophils are still largely unknown. In our study, the observation of association between different isoforms of *HIF-1A* and distinct physiological phenotypes may therefore fill this gap. Importantly, our findings highlight that therapeutic target in PM-induced diseases should be targeted at a specific isoform dependent on physiological phenotypes rather than a whole gene.

5. Conclusion

We found that BRs exclusively expressed PM-associated isoforms (PMAIs) of PFKFB3 and LDHA, encoding two key enzymes responsible for stimulating and maintaining glycolysis, respectively. PMAIs of PFKFB3 were expected to stimulate glycolysis in different sub-cellular functional compartments to trigger different immune functions sub-cellularly. PMAIs of LDHA have longer 3'UTRs relative to the one expressed in CRs, which enhance LDHA mRNA stability and translational efficiency, thus allowing glycolysis maintenance. The regulation of alternative splicing of both genes were directly regulated by different HIF-1A and HIF-1B isoforms. Importantly, these different isoforms could explain large variances of different physiological phenotypes, providing molecular evidence linking air pollution exposure and physiological phenotypes. Remarkably, AS of HIF-1A and PFKFB3 were significantly suppressed and expression of both genes was downregulated in COPD (Chronic Obstructive Pulmonary Disease) patients compared with BRs, suggesting that HIF-1 mediated defective glycolysis mediate neutrophil dysfunction, leading to subsequent progression of PM-induced diseases.

Supplementary Materials: The following are available online at www.mdpi.com/xxx/s1.

Author Contributions: Conceptualization, X.Z. and K.B.; Methodology, X.Z., K.B., S.P., X.F., R.A, T.P., Y.W., Z.L., F.X, C.J.; Data Analysis, S.P., D.P., K.B., R.A., T.P., X.D.; Writing (original draft), K.B., S.P.; Writing (review and editing), all co-authors; Funding Acquisition, K.B. and X. Z.

Data Availability: The raw sequencing data have been deposited in http://bigd.big.ac.cn/.

ACKNOWLEDGEMENTS: This study was supported by, the Strategic Priority Program of the Chinese Academy of Sciences (XDB31000000), Newton Advanced Fellowship to X.Z., and Youth Innovation Promotion Association of Chinese Academy of Sciences (2020086), the National Key Research and Development Program (2016YFC1304603).

Conflicts of Interest: The authors declare no competing interests. All procedures followed were in accordance with the ethical standards of the responsible committee on human experimentation (institutional and national) and with the Helsinki Declaration of 1975, as revised in 2000 (5). Informed consent was obtained from all patients for being included in the study.

References

1. World Health Organization. (2016). Ambient air pollution: a global assessment of exposure and burden of disease. World Health Organization. https://apps.who.int/iris/handle/10665/250141-eng.pdf.
2. Brook, R.D., Rajagopalan, S., Pope 3rd, C.A., Brook, J.R., Bhatnagar, A., Diez-Roux, A.V., Holguin, F., Hong, Y., Luepker, R.V., Mittleman, M.A., et al. (2010). Particulate matter air pollution and cardiovascular disease: an update to the scientific statement from the American Heart Association. Circulation 121, 2331-7238.
3. Zhao, J., Li, M., Wang, Z., Chen, J., Zhao, J., Xu, Y., Wei, X., Wang, J., and Xie, J. (2019). Role of PM2.5 in the development and progression of COPD and its mechanisms. Respir. Res. *20*, 120.
4. Feng, X., Shao, L., Xi, C., Jones, T., Zhang, D., and BéruBé, K. (2020). Particle-induced oxidative damage by indoor size-segregated particulate matter from coal-burning homes in the Xuanwei lung cancer epidemic area, Yunnan Province, China. Chemosphere *256*, 127058.
5. Yan, Y.H., Chou, C.C.K., Wang, J.S., Tung, C.L., Li, Y.R., Lo, K., and Cheng, T.J. (2014). Subchronic effects of inhaled ambient particulate matter on glucose homeostasis and target organ damage in a type 1 diabetic rat model. Toxicol. Appl. Pharmacol. *281*, 211-220.
6. World Health Organization. WHO Global Urban Ambient Air Pollution Database (Update 2016) [WWW Document], WHO http://www.who.int/phe/health_topics/outdoorair/databases/cities/en/ accessed 10.10.17.
7. Li, T., Hu, R., Chen, Z., Li, Q., Huang, S., Zhu, Z., and Zhou, L.F. (2018). Fine particulate matter (PM2.5): The culprit for chronic lung diseases in China. Chronic Dis. Transl. Med. *4*, 176-186.
8. Price, H.D., Jones, T.P., and BéruBé, K.A. (2014). Resolution of the mediators of in vitro oxidative reactivity in size-segregated fractions that may be masked in the urban PM(10) cocktail. Sci. Total. Environ. *485-486*, 588-595.
9. Adams, R. (2014). Training response inhibition to reduce food consumption. PhD Thesis, Cardiff University.
10. Chuang, H.C., Jones. T.P., Chen, T.T., and BéruBé, K.A. (2013). Cytotoxic effects of incense particles in relation to oxidative stress, the cell cycle and F-actin assembly. Toxicol. Lett. *220*, 229-237.
11. Chuang, H.C., BéruBé, K.A., Lung, S.C., Bai, K.J., and Jones, T.P. (2013). Investigation into the oxidative potential generated by the formation of particulate matter from incense combustion. J. Hazard. Mater. *244-245*, 142-150.
12. Huttunen, K., Wlodarczyk, A.J., Tirkkonen, J., Mikkonen, S., Täubel, M., Krop, E., Jacobs J., Pekkanen, J., Heederik, D., Zock, J.P., et al. (2019). Oxidative capacity and haemolytic activity of settled dust from moisture-damaged schools. Indoor Air *29*, 299-307.
13. Shao, L., Hou, C., Geng, C., Liu, J., Hu, Y., Wang, J., Jones, T., Zhao, C., and Berube, K. (2015). The oxidative potential of PM10 from coal, briquettes and wood charcoal burnt in an experimental domestic stove. Atmos. Environ. *127*, 372-381.
14. Shao, L., Hu, Y., Shen, R., Schäfer, K., Wang, J., Wang, J., Schnelle-Kreis, J., Zimmermann, R., BéruBé, K., and Suppan, P. (2017). Seasonal variation of particle-induced oxidative potential of airborne particulate matter in Beijing. Sci. Total. Environ. *579*, 1152-1160.
15. Jones, T.P., and Bérubé, K.A. (2011). The bioreactivity of the sub-10 μm component of volcanic ash: Soufrière Hills volcano, Montserrat. J. Hazard. Mater. *194*, 128-134.
16. Chen, T, Chuang, K.J., Chiang, L.L., Chen, C.C., Yeh, C.T., Wang, L.S., Gregory, C., Jones, T., BéruBé, K., Lee, C.N., et al. (2014). Characterization of the interactions between protein and carbon black. J. Hazard. Mater. *264*, 127-135.
17. Moreno, T., Martins, V., Querol, X., Jones, T., BéruBé, K., Minguillón, M.C., Amato, F., Capdevila, M., de Miguel, E., Centelles, S., et al. (2015). A new look at inhalable metalliferous airborne particles on rail subway platforms. Sci. Total Environ. *505*, 367-375.
18. Pope, C.A., 3rd, Burnett, R.T., Thurston, G.D., Thun, M.J., Calle, E.E., Krewski, D., and Godleski, J.J. (2004). Cardiovascular mortality and long-term exposure to particulate air pollution-epidemiological evidence of general pathophysiological pathways of disease. Circulation *109*, 71-77.
19. Injarabian, L., Devin, A., Ransac, S., and Marteyn, B.S. (2020). Neutrophil metabolic shift during their lifecycle: Impact on their survival and activation. Int. J. Mol. Sci. *21*, 287.
20. Wright, H.L., Moots, R.J., Bucknall, R.C., and Edwards, S.W. (2010). Neutrophil function in inflammation and inflammatory diseases. Rheumatology *49*, 1618-1631.
21. Weiss, D.J., and Klausner, J.S. (1988). Neutrophil-induced erythrocyte injury: a potential cause of erythrocyte destruction in the anemia associated with inflammatory disease. Vet. Pathol. *25*, 450-455.

22. Meinderts, S.M., Oldenborg, P.A., Beuger, B.M., Klei, T., Johansson, J., Kuijpers, T.W., Matozaki, T., Huisman, E.J., de Haas, M., van den Berg, T.K., et al. (2017). Human and murine splenic neutrophils are potent phagocytes of IgG-opsonized red blood cells. Blood Adv. *1*, 875-886.
23. Peretz, A., Peck, E.C., Bammler, T.K., Beyer, R.P., Sullivan, J.H., Trenga, C.A., Srinouanprachnah, S., Farin, F.M., and Kaufman, J.D. (2007). Diesel exhaust inhalation and assessment of peripheral blood mononuclear cell gene transcription effects: an exploratory study of healthy human volunteers. Inhal. Toxicol. *19*, 1107-1119.
24. Zhou, Z., Liu, Y., Duan, F., Qin, M., Wu, F., Sheng, W., Yang, L., Liu, J., and He, K. (2015). Transcriptomic analyses of the biological effects of airborne PM2.5 exposure on human bronchial epithelial cells. PLoS One *10*, e0138267.
25. Líbalová, H., Uhlířová, K., Kléma, J., Machala, M., Šrám, R. J., Ciganek, M., amd Topinka, J. (2012). Global gene expression changes in human embryonic lung fibroblasts induced by organic extracts from respirable air particles. Part. Fibre. Toxicol. *9*, 1.
26. Watterson, T.L., Sorensen, J., Martin, R., and Coulombe, R.A. (2007). Effects of PM2.5 collected from Cache Valley Utah on genes associated with the inflammatory response in human lung cells. J. Toxicol. Environ. Health A. *70*, 1731-1744.
27. Zhang, H., Yuan, H., Liu, X., Yu, J., and Jiao Y. (2018). Impact of synoptic weather patterns on 24 h-average PM2.5 concentrations in the North China Plain during 2013-2017. Sci. Total Environ. *627*, 200-210.
28. Shao, L., Shi, Z., Jones, T.P., Li, J., Whittaker, A.G., and Bérubé, K.A. (2006). Bioreactivity of particulate matter in Beijing air: results from plasmid DNA assay. Sci. Total Environ. *367*, 261-272.
29. Shi, Z., Shao, L., Jones, T., Whittaker, A. G., Lu, S., Berube, K., He T., and Richards, R. (2003). Characterization of airborne individual particles collected in an urban area, a satellite city and a clean air area in Beijing, 2001. Atmos. Environ. *37*, 4047-4108.
30. Lu, S., Shao, L., Wu, M., Jones, T.P., Merolla, L., and Richard, R.J. (2006). Correlation between plasmid DNA damage induced by PM and trace metals in inhalable particulate matters in Beijing air. Sci. Chinan Ser. D. Earth Sci. *49*,1323-1331.
31. Shao, L., Li, J., Zhao, H., Yang, S., Li, H., Li, W., Jones, T., Sexton, K., and BéruBé, K. (2007). Associations between particle physicochemical characteristics and oxidative capacity: An indoor PM10 study in Beijing, China. Atmos. Environ. *41*, 5316-5326.
32. Jones, T., Wlodarczyk, A., Koshy, L., Brown, P., Shao, L., and BéruBé, K. (2009). The geochemistry and bioreactivity of fly-ash from coal-burning power stations. Biomarkers *14*, 45-48.
33. Shi, Z., Shao, L., Li, H., Whittaker, A.G., Jones, T.P., BeruBe, K.A., and Richards, R.J. (2002). Physicochemical characterization of the PM10 in ambient air of northwestern Beijing urban area during heating-period. Huan Jing Ke Xue *23*, 30-34.
34. Shi, Z., Shao, L., Jones, T.P., and Lu, S. (2005). Microscopy and mineralogy of airborne particles collected during severe dust storm episodes in Beijing, China. J. Geophys. Res. *110*, 1-10.
35. Whittaker, A.G., Jones, T.P., Shao, L., Shi, Z., Berube, K., and Richards, R.J. (2003). Mineral dust in urban air: Beijing, China. Mineral. Mag. *67*,173-182.
36. Yuan, G., and Yang, W. (2019). Evaluating China's air pollution control policy with extended AQI indicator system: example of the Beijing-Tianjin-Hebei region. Sustainability *11*, 93.
37. Miller, M. R., Crapo, R., Hankinson, J., Brusasco, V., Burgos, F., Casaburi, R., Coates, A., Enright, P., van der Grinten, C. P., Gustafsson, P., et al. (2005). General considerations for lung function testing. Eur. Respir. J. *26*, 153-161.
38. Piorunek, T., Kostrzewska, M., Cofta, S., Batura-Gabryel, H., Andrzejczak, P., Bogdański, P., and Wysocka, E. (2015). Impulse oscillometry in the diagnosis of airway resistance in chronic obstructive pulmonary disease. Adv. Exp. Med. Biol. 838, 47-52.
39. Kim, D., Langmead, B., amd Salzberg, S.L. (2015). HISAT: a fast spliced aligner with low memory requirements. Nat. Method *12*, 357-360.
40. Pertea, M., Pertea, G.M., Antonescu, C.M., Chang, T.C., Mendell, J.T., and Salzberg, S.L. (2015). StringTie enables improved reconstruction of a transcriptome from RNA-seq reads. Nat. biotechnol. *33*, 290-295.
41. Li, B., and Dewey, C.N. (2011). RSEM: accurate transcript quantification from RNA-Seq data with or without a reference genome. BMC Bioinformatics *12*, 323.
42. Cartegni, L., Wang, J., Zhu, Z., Zhang, M.Q., and Krainer, A.R. (2003). ESEfinder: a web resource to identify exonic splicing enhancers. Nucleic Acid Res. *31*, 3568-3571.
43. Pan, S., Zhang, T., Rong, Z., Hu, L., Gu, Z., Wu, Q., Dong, S., Liu, Q., Lin, Z., Deutschova, L., et al. (2017). Population transcriptomes reveal synergistic responses of DNA polymorphism and RNA expression to extreme environments on the Qinghai-Tibetan Plateau in a predatory bird. Mol. Ecol. *26*, 2993-3010.
44. Zhou, X. B., Lindsay, H., and Robinson, M.D. (2014). Robustly detecting differential expression in RNA sequencing data using observation weights. Nucleic Acids Res. *42*, e91.
45. Anders, S., and Huber, W. (2010). Differential expression analysis for sequence count data. Genome Biol. *11*, R106.
46. Li, J., and Tibshirani, R. (2013). Finding consistent patterns: a nonparametric approach for identifying differential expression in RNA-Seq data. Stat. Methods Med. Res. *22*, 519-523.
47. Smyth, G.K. (2004). Linear models and empirical Bayes methods for assessing differential expression in microarray experiments. Stat. Appl. Genet. Mol. Biol. *3*, 3.
48. Mor, I., Cheung, E.C., and Vousden, K.H. (2011). Control of glycolysis through regulation of PFK1: old friends and recent additions. Cold Spring Harb. Symp. Quant. Biol. *76*, 211-216.
49. Martinez-Contreras, R., Cloutier, P., Shkreta, L., Fisette, J.F., Revil, T., and Chabot, B. (2007). hnRNP proteins and splicing control. Adv. Exp. Med. Biol. *623*, 123-147.
50. Zhou, Z., and Fu, X.D. (2013). Regulation of splicing by SR proteins and SR protein-specific kinases. Chromosoma *122*, 191-207.

51. Jian, X., Boerwinkle, E., and Liu, X. (2014). In silico tools for splicing defect prediction: a survey from the viewpoint of end users. Genet. Med. *16*, 497-503.
52. Chen, C.D., Kobayashi, R., and Helfman, D.M. (1999). Binding of hnRNP H to an exonic splicing silencer is involved in the regulation of alternative splicing of the rat beta-tropomyosin gene. Genes Dev. *13*, 593-606.
53. Han, G., Lu, C., Guo, J., Qiao, Z., Sui, N., Qiu, N., and Wang, B. (2020). C2H2 Zinc finger proteins: master regulators of abiotic stress responses in plants. Front. Plant Sci. *11*, 115.
54. Cassandri, M., Smirnov, A., Novelli, F., Pitolli, C., Agostini, M., Malewicz, M., Melino, G., and Raschellà, G. (2017). Zinc-finger proteins in health and disease. Cell Death Discov. *3*, 17071.
55. Dai, J., Sun, C., Yao, Z., Chen, W., Yu, L., and Long, M. (2016). Exposure to concentrated ambient fine particulate matter disrupts vascular endothelial cell barrier function via the IL-6/HIF-1α signaling pathway. FEBS Open Bio. *6*, 720-728.
56. Cramer, T., Yamanishi, Y., Clausen, B. E., Förster, I., Pawlinski, R., Mackman, N., Haase, V. H., Jaenisch, R., Corr, M., Nizet, V., et al. (2003). HIF-1a is essential for myeloid cell-mediated inflammation. Cell *112*, 645-657.
57. Egners, A., Erdem, M., and Cramer, T. (2016). The response of macrophages and neutrophils to hypoxia in the context of cancer and other inflammatory diseases. Mediators Inflamm. *2016*, 2053646.
58. Sun, L., Fu, J., Lin, S. H., Sun, J. L., Xia, L., Lin, C. H., Liu, L., Zhang, C., Yang, L., Xue, P., et al. (2020). Particulate matter of 2.5 μm or less in diameter disturbs the balance of TH17/regulatory T cells by targeting glutamate oxaloacetate transaminase 1 and hypoxia-inducible factor 1α in an asthma model. J. Allergy Clin. Immunol. *145*, 402-414.
59. Li, H., Cai, J., Chen, R., Zhao, Z., Ying, Z., Wang, L., Chen, J., Hao, K., Kinney, P.L., Chen, H., et al. (2017). Particulate matter exposure and stress hormone levels: a randomized, double-blind, crossover trial of air purification. Circulation *136*, 618-627.
60. Yi, M., Ban, Y., Tan, Y., Xiong, W., Li, G., and Xiang, B. (2019). 6-Phosphofructo-2-kinase/fructose-2,6-biphosphatase 3 and 4: A pair of valves for fine-tuning of glucose metabolism in human cancer. Mol. Metab. *20*,1-13.
61. Kim, S.G., Manes, N.P., El-Maghrabi, M.R., and Lee, Y.H. (2006). Crystal structure of the hypoxia-inducible form of 6-phosphofructo-2-kinase/fructose-2,6-bisphosphatase (PFKFB3): a possible new target for cancer therapy. J. Biol. Chem. *281*, 2939-2944.
62. Minchenko, O.H., Ogura, T., Opentanova, I.L., Minchenko, D.O., and Esumi, H. (2005). Splice isoform of 6-phosphofructo-2-kinase/fructose-2,6-bisphosphatase-4: expression and hypoxic regulation. Mol. Cell. Biochem. *280*, 227-234.
63. Semenza, G.L., Jiang, B.H., Leung, S.W., Passantino, R., Concordet, J.P., Maire, P., and Giallongo, A. (1996). Hypoxia response elements in the aldolase A, enolase 1, and lactate dehydrogenase A gene promoters contain essential binding sites for hypoxia-inducible factor 1. J Biol. Chem. *271*, 32529-32537.
64. Tanguay, R.L., and Gallie, D.R. (1996). Translational efficiency is regulated by the length of the 3' untranslated region. Mol. Cell Biol. *16*, 146-156.
65. Zhao, R.Z., Jiang, S., Zhang, L., and Yu, Z.B. (2019). Mitochondrial electron transport chain, ROS generation and uncoupling (Review). Int. J. Mol. Med. *44*, 3-15.
66. Sanders, L.H., and Greenamyre, T.J. (2013). Oxidative damage to macromolecules in human Parkinson disease and the rotenone model. Free Radic. Biol. Med. *62*, 111-120.
67. Minchenko, A., Leshchinsky, I., Opentanova, I., Sang, N., Srinivas, V., Armstead, V., and Caro, J. (2002). Hypoxia-inducible factor-1-mediated expression of the 6-phosphofructo-2-kinase/fructose-2,6-bisphosphatase-3 (*PFKFB3*) gene. Its possible role in the Warburg effect. J. Biol. Chem. *277*, 6183-6187.
68. Cui, X.G., Han, Z.T., He, S.H., Wu, X.D., Chen, T.R., Shao, C.H., Chen, D.L., Su, N., Chen, Y.M., Wang, T., et al. (2017). HIF1/2α mediates hypoxia-induced LDHA expression in human pancreatic cancer cells. Oncotarget. *8*, 24840-24852.
69. Greijer, A.E., and van der Wall, E. (2004). The role of hypoxia inducible factor 1 (HIF-1) in hypoxia induced apoptosis. J. Clin. Pathol. *57*, 1009-1014.
70. Zhao, J., Zhou, Y., Zhang, X., and Chen, L. (2016). Part mutual information for quantifying direct associations in networks. Proc. Natl. Acad. Sci. USA. *113*, 5130-5135.
71. Anderson, J.M., Rodriguez, A., and Chang, D.T. Foreign body reaction to biomaterials. Semin. Immunol. *20*, 86-100 (2008).
72. McCracken, J.M., and Allen, L.A. (2014). Regulation of human neutrophil apoptosis and lifespan in health and disease. J. Cell Death *7*, 15-23.
73. Volpe, E., Sambucci, M., Battistini, L., and Borsellino, G. (2016). Fas-Fas Ligand: checkpoint of T cell functions in multiple sclerosis. Front. Immunol. *7*, 382.
74. Selders, G.S., Fetz, A.E., Radic, M.Z., and Bowlin, G.L. (2017). An overview of the role of neutrophils in innate immunity, inflammation and host-biomaterial integration. Regen. Biomater. *4*, 55-68.
75. Hou, G., Valujskikh, A., Bayer, J., Stavitsky, A.B., Metz, C., and Heeger, P.S. (2001). In vivo blockade of macrophage migration inhibitory factor prevents skin graft destruction after indirect allorecognition. Transplantation *72*, 1890-1897.
76. Demir, Y., Chen, Y., Metz, C., Renz, H., and Heeger, P.S. (2003). Cardiac allograft rejection in the absence of macrophage migration inhibitory factor. Transplantation *76*, 244-247.
77. Huang, X.R., Chun Hui, C.W., Chen, Y.X., Wong, B.C., Fung, P.C., Metz, C., Cho, C.H., Hui, W.M., Bucala, R., Lam, S.K., et al. (2001). Macrophage migration inhibitory factor is an important mediator in the pathogenesis of gastric inflammation in rats. Gastroenterology. *121*, 619-630.

78. Ferro, E.A., Mineo, J.R., Ietta, F., Bechi, N., Romagnoli, R., Silva, D.A., Sorda, G., Bevilacqua, E., and Paulesu, L.R. (2008). Macrophage migration inhibitory factor is up-regulated in human first-trimester placenta stimulated by soluble antigen of Toxoplasma gondii, resulting in increased monocyte adhesion on villous explants. Am. J. Pathol. *172*, 50-58.
79. Jovanović, M., and Vićovac, L. (2009). Interleukin-6 stimulates cell migration, invasion and integrin expression in HTR-8/SVneo cell line. Placenta *30*, 320-328.
80. Lei, C.T., Su, H., Ye, C., Tang, H., Gao, P., Wan, C., He, F.F., Wang, Y.M., and Zhang, C. (2018). The classic signalling and trans-signalling of interleukin-6 are both injurious in podocyte under high glucose exposure. J. Cell Mol. Med. *22*, 251-260.
81. Maston, L.D., Jones, D.T., Giermakowska, W., Resta, T.C., Ramiro-Diaz, J., Howard, T.A., Jernigan, N.L., Herbert, L., Maurice, A.A., and Gonzalez Bosc, L.V. (2018). Interleukin-6 trans-signaling contributes to chronic hypoxia-induced pulmonary hypertension. Pulm. Circ. *8*, 2045894018780734.
82. Stringer, K.A., Tobias, M., O'Neill, H.C., and Franklin, C.C. (2007). Cigarette smoke extract-induced suppression of caspase-3-like activity impairs human neutrophil phagocytosis. Am. J. Physiol. Lung Cell Mol. Physiol. *292*, 1572-1579.
83. McGovern, N.N., Cowburn, A.S., Porter, L., Walmsley, S.R., Summers, C., Thompson, A., Anwar, S., Willcocks, L.C., Whyte, M., Condliffe, A.M., et al. (2011). Hypoxia selectively inhibits respiratory burst activity and killing of Staphylococcus aureus in human neutrophils. J. Immunol. *186*, 453-463.
84. Drannik, A.G., Pouladi, M.A., Robbins, C.S., Goncharova, S.I., Kianpour, S., and Stämpfli, M.R. (2004). Impact of cigarette smoke on clearance and inflammation after *Pseudomonas aeruginosa* infection. Am. J. Respir. Crit. Care Med. *170*, 1164-1171.
85. Sapey, E., Stockley, J.A., Greenwood, H., Ahmad, A., Bayley, D., Lord, J.M., Insall, R. H., and Stockley, R.A. (2011). Behavioral and structural differences in migrating peripheral neutrophils from patients with chronic obstructive pulmonary disease. Am. J. Respir. Crit. Care Med. *183*, 1176-1186.
86. Jeong, S., Park, S.A., Park, I., Kim, P., Cho, N.H., Hyun, J.W., and Hyun, Y.M. (2019). PM2.5 exposure in the respiratory system induces distinct inflammatory signaling in the lung and the liver of mice. J. Immunol. Res. *2019*, 3486841.
87. Sun, Q., Jiang, S., and Xu, X. (2012). Particulate air pollution on systemic inflammatory response: roles of monocytes and neutrophils. Eur. Respir. J. *40*, 4783.
88. Hoenderdos, K., and Condliffe, A. (2013). The neutrophil in Chronic Obstructive Pulmonary Disease. Too little, too late or too much, too soon? Am. J. Respir. Cell Mol. Biol. *48*, 531-539.
89. Alberts, N., Johnson, A., Lewis, J., Raff, M., Roberts, K., and Walter, P. (2002). Molecular Biology of the Cell. 4th edition. (New York: Garland Science).
90. Wang, A., Huen, S.C., Luan, H.H., Yu, S., Zhang, C., Gallezot, J.D., Booth, C.J., and Medzhitov, R. (2016). Opposing effects of fasting metabolism on tissue tolerance in bacterial and viral inflammation. Cell *166*, 1512-1525.
91. Bowden, S.D., Rowley, G., Hinton, J.C., and Thompson, A. (2009). Glucose and glycolysis are required for the successful infection of macrophages and mice by *Salmonella enterica Serovar Typhimurium*. Infect. Immun. *77*, 3117-3126.
92. Xavier, M.N., Winter, M.G., Spees, A.M., den Hartigh, A.B., Nguyen, K., Roux, C.M., Silva, T.M., Atluri, V.L., Kerrinnes, T., Keestra, A.M., et al. (2013). PPARγ-mediated increase in glucose availability sustains chronic Brucella abortus infection in alternatively activated macrophages. Cell Host Microbe *14*, 159-170.
93. Reyes-Caballero, H., Rao, X., Sun, Q., Warmoes, M.O., Lin, P., Sussan, T.E., Park, B., Fan, T.W.M., Maiseyeum, A., Rajagopalan, S., et al. (2019) Air pollution-derived particulate matter dysregulates hepatic Krebs cycle, glucose and lipid metabolism in mice. Sci. Rep. *9*, 17423.